A more effective rationalisation of fatigue crack growth rate data for various specimen geometries and stress ratios using the CJP model

Yang, B

A more effective rationalisation of fatigue crack growth rate data for various specimen geometries and stress ratios using the CJP model

Bing Yang [♣][1], M N James [2, 3, *]

[1] State Key Laboratory of Traction Power, Southwest Jiaotong University, Chengdu, China.

[2] School of Engineering, University of Plymouth, Plymouth, England.

[3] Department of Mechanical Engineering, Nelson Mandela Metropolitan University, Port Elizabeth, South Africa.

* Corresponding author: mjames@plymouth.ac.uk

Abstract

This paper explores the capability of the effective stress intensity factor range, ΔK_{CJP}, which is derived from the CJP model of crack tip stresses, to provide a better rationalisation of fatigue crack growth rate across several specimen geometries and stress ratios, than the standard definition of ΔK_{eff}. It takes both the stress intensity factor, K_F that drives crack growth and the stress intensity factor, K_R that acts to retard crack growth into account, and is defined as $(K_{F, max}-K_{R, max})-(K_{F, min}-K_{R, min})$. The fatigue crack growth rate tests using Grade 2 titanium CT specimens and DEN specimens at different stress ratios were carried out and the crack tip displacement fields were measured using digital image correlation (DIC) technique. Test results reveal that compared to the data of da/dN vs. standard ΔK on log-log coordinate graph, the data of da/dN vs. ΔK_{CJP} for various specimen geometries and stress ratios actually distributes along a straight line within a narrow-band. The ΔK_{CJP}

[♣]   This work was performed while Bing Yang was a Visiting Researcher at the University of Plymouth

shows its distinct stress ratio-independent and geometry-independent characteristics. A da/dN-ΔK_{CJP} equation for the titanium in this study was then obtained. Furthermore, to facilitate the application of the CJP model, the relations between ΔK_{CJP} and ΔK were determined by constructing the calibration curves for relating the constants in the CJP model to the standard ΔK. Therefore, ΔK_{CJP} is applicable for a more effective rationalisation of fatigue crack growth rate for various specimen geometries and tress ratios.

Keywords: crack tip displacement fields, digital image correlation, stress intensity factor range, calibration curve, fatigue.

1. Experimental work

The experimental work was carried out using three compact tension (CT) specimens and two double edge notched (DEN) specimens (Fig. 1) which were manufactured from a 1 mm thick sheet of commercially pure grade 2 titanium. Table 1 gives the test conditions for present fatigue tests. The CT specimens were subjected to constant amplitude fatigue loading under stress ratio, R, of 0.1, 0.3 and 0.6 respectively with a fixed maximum load of 700N, while for the DEN specimens the stress ratios were 0.05, 0.3 and the maximum load is 2200N. The loading frequency, f, is 10 Hz and the loading mode is sine wave. The chemical composition and the mechanical properties of this commercially pure titanium alloy are presented respectively in Tables 2 and 3.

The two surfaces of each specimen were treated using different methods to facilitate the digital image correlation (DIC) study and the crack length measurements. The surface utilized for DIC study was sprayed random black speckle pattern over a white background, while the other surface of the specimen was grinded and polished so as to track the crack tip position more easily with a travelling microscope which has a precision of 10 μm.

All the fatigue crack growth tests were conducted on an ElectroPuls E3000 dynamic testing machine (Fig. 2). A 1/2" monochrome progressive scan CCD camera equipped with a 10× macro-zoom lens (MLH-10×) was placed perpendicular to the speckled surface of the specimen to provide the necessary spatial resolution in the measurement region surrounding the crack tip. The field of view was 1624 pixels by 1202 pixels. However due to the inevitable difference caused by the focusing process for each specimen, the spatial resolutions (also listed in Table 1) are more or less different among the specimens. During

fatigue testing, a sequence of images was captured at different load levels (including but not limited to the maximum load, the minimum load and the mean load) through complete loading and unloading cycles; this involved periodically pausing the fatigue cycling and applying stepwise loading through a fatigue cycle making measurements at each step. When the fatigue cycling was paused, the crack tip position was recorded using the travelling microscope for calculating the crack length. The crack path was located to be at the centre of the image and the speckled surface of the specimens was illuminated with a high intensity LED (also shown in Fig. 2).
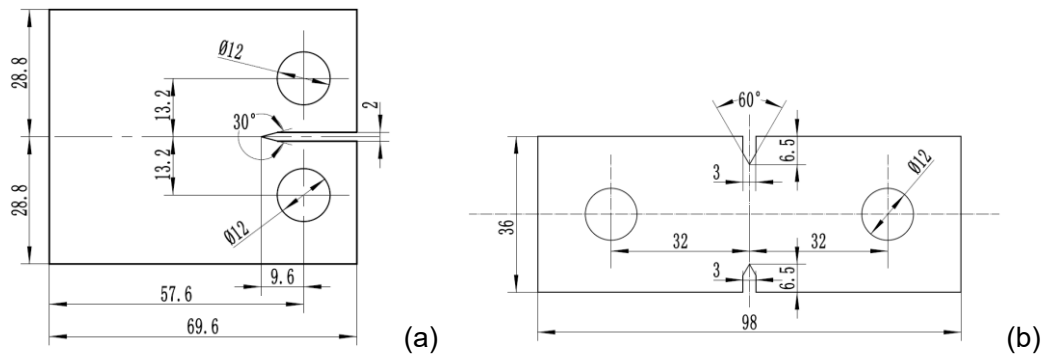

Fig. 1. Geometry and dimensions (mm) of the specimens used in this study. (a) CT specimen and (b) DEN specimen.
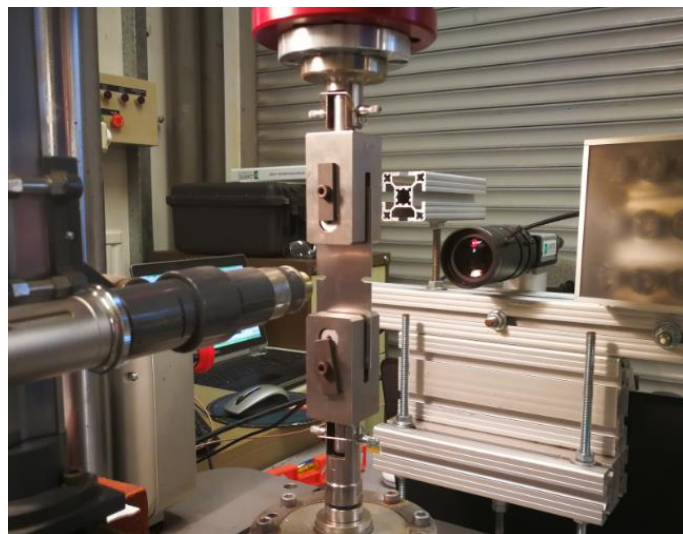
Fig. 2. Test setup used to measure displacement fields by DIC and to track the crack tip position during fatigue testing

Table 1. Test conditions for the fatigue tests.

Specimen No.	Loading conditions				Spatial resolution (µm/pixel)
	P_{max} (N)	R	f (Hz)	Wave mode	
CT1	700	0.1	10	sine	8.33
CT2	700	0.3	10	sine	8.33
CT3	700	0.6	10	sine	8.22
DEN1	2200	0.05	10	sine	8.62
DEN2	2200	0.3	10	sine	8.61

Table 2. Chemical composition (wt.%).

Element	Fe	C	N	O	H	Titanium
Requirement	<0.20	≤0.08	≤0.05	≤0.20	≤0.015	remainder
Result	0.10	0.01	<0.01	0.12	0.002	remainder

Table 3. Mechanical properties.

Parameter	E (MPa)	σ_b (MPa)	σ_s (MPa)	δ (%)	v
Value	105000	448	390	20	0.33

2. Description of fatigue crack growth rate using different stress intensity factor range

Standard Irwin stress intensity factor range, ΔK, is considered to be a relatively rational parameter to represent the crack growth driving force. However, Irwin ΔK-value is sensitive to stress ratio and also to specimen geometry, which means once the loading condition or the specimen geometry changes, the expression of ΔK need to be amended accordingly. Based on the CJP model, a new stress intensity factor range, ΔK_{CJP}, can provide a better rationalisation of crack growth rate across different stress ratios and several specimen geometries. This section introduces the standard Irwin ΔK-value for the CT and the DEN

specimens and the definition of the CJP model-based ΔK_{CJP}-value, and then demonstrates

the description effects to test data of fatigue crack growth rate by taking ΔK and ΔK_{CJP} as

the driving force respectively.

2.1. Definitions of ΔK and ΔK_{CJP}

2.1.1. ΔK for CT specimen

For CT specimen, the solution for the theoretical value of stress intensity factor range, ΔK,

can be given by [1]:

$$\Delta K = \frac{P_{max} - P_{min}}{t\sqrt{b}} \times \frac{\left(2 + \dfrac{a}{b}\right)}{\left(1 - \dfrac{a}{b}\right)^{3/2}} \times 2 \times F_2\left(\frac{a}{b}, \frac{h}{b}, \frac{d}{h}\right) \tag{1}$$

where, P_{max} and P_{min} are the maximum load and the minimum applied load; t, b, h and d

are the thickness, the width, the half-height and the distance from notch surface to hole

edge of the specimen respectively (Fig. 3); a is the crack length measured from the centre

of the pin holes; F_2 is a non-dimensional function of (a/h, h/b, d/h) which can be estimated
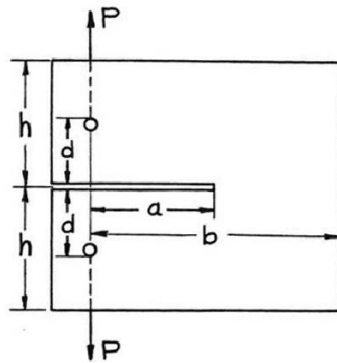
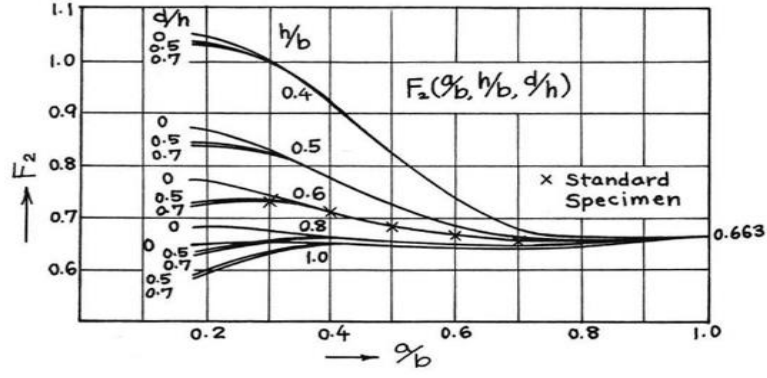from Fig. 3b.

Fig. 3. Sketch of CT specimen [1]

Fig. 4. Numerical value curves of function F_2 [1]

It can be seen from Fig. 1a that the value of h/b for the CT specimen in present study is 0.5, which has longer ligament to allow greater stable crack propagation than that in standard CT specimen (h/b=0.6). The curve of F_2 according to h/b=0.5 can be digitized as following quartic equation:

$$F_2 = 0.681 + 1.89(a/b) - 6.94(a/b)^2 + 8.27(a/b)^3 - 3.25(a/b)^4 \tag{2}$$

Hence, ΔK for present CT specimen can be depicted as:

$$\Delta K = \frac{P_{max} - P_{min}}{t\sqrt{b}} \times \frac{\left(2 + \dfrac{a}{b}\right)}{\left(1 - \dfrac{a}{b}\right)^{3/2}} \times \left[1.362 + 3.78\left(\frac{a}{b}\right) - 13.88\left(\frac{a}{b}\right)^2 + 16.54\left(\frac{a}{b}\right)^3 - 6.5\left(\frac{a}{b}\right)^4\right] \tag{3}$$

2.1.2. ΔK for DEN specimen

For DEN specimen, the solution for ΔK can be given by [2]:

$$\Delta K = \frac{P_{max} - P_{min}}{2W \times t}\sqrt{\pi a}\,\frac{1.122 - 0.561(\alpha) - 0.015\alpha^2 + 0.091\alpha^3}{\sqrt{1-\alpha}} \tag{4}$$

where, W and t are the half-width and the thickness of the specimen respectively (Fig. 5); a is the crack length measured from the edge of the notch; α is the ratio of a to W.
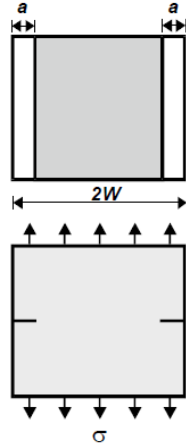
Fig. 5. Sketch of DEN specimen [2]

2.1.3. Definition of ΔK_{CJP}

CJP model [3] has defined two new primary stress intensity factors K_F and K_R. K_F is the stress intensity factor that drives crack growth and K_R is the stress intensity factor that acts to retard crack growth. The difference between the two stress intensity factors explicitly provides the effective crack driving force, and thus a new CJP model-based stress intensity factor range can be defined as:

$$\Delta K_{\mathrm{CJP}} = \left(K_{F,\mathrm{max}} - K_{R,\mathrm{max}} \right) - \left(K_{F,\mathrm{min}} - K_{R,\mathrm{min}} \right) \tag{5}$$

The CJP model considers that the plastic enclave surrounding a fatigue crack acts to shield it from the full influence of the elastic stress field that drives the fatigue crack growth and that these plasticity-induced effects can be assessed from consideration of the elastic field. Because the model is only valid in the near-tip elastic field region, it is important to identify a suitable DIC analysis region surrounding the crack tip where the plastic zone can be removed while the valid experimental data size is relatively stable to ensure the consistency of the calculation results. For present study, the analysis region is illustrated as shown in Fig. 6. An inner radius of 0.5 mm is set to avoid the possible influence of plastic

deformation at the crack tip and an outer radius of 2 mm is defined to be within the region

dominated by the elastic zone. Specially, when the crack length is less than 2 mm, the

wake length is set to be the crack length. The vertical displacement field is adopted to

determine the accurate position of the crack tip by finding the demarcation point between

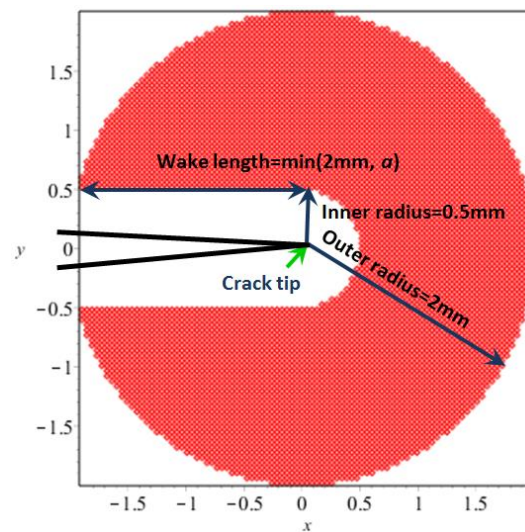the sudden change and the continuous change of the vertical displacement.

Fig. 6. Definition of the DIC analysis region surrounding the crack tip

2.2. Comparisons between the fatigue crack growth rate relations

2.2.1. The da/dN-ΔK and the da/dN-ΔK_{CJP} relations for CT specimens

Test data of the da/dN-ΔK and that of the da/dN-ΔK_{CJP} for CT specimens on log-log

coordinate graphs are shown in Fig. 7. Though the commercially pure titanium alloy applied

in this study shows less obvious plasticity-induced shielding effect on fatigue crack growth

of CT specimens, it still indicates from Fig. 7a that with the increase of R, the da/dN-ΔK

data shows a relatively higher growth rate at the same given ΔK value. However as shown

in Fig. 7b, test data of da/dN-ΔK_{CJP} obtained from all the three CT specimens seemingly

distributes along a rather straight line in the graph on log-log axes and just overlap with

one another with the same ΔK_{CJP} value range. This indicates the CJP model-based stress

intensity factor range, ΔK_{CJP}, is a more effective range which can be obtained immediately

without measurements of plasticity-induced shielding, which makes it a stress ratio-
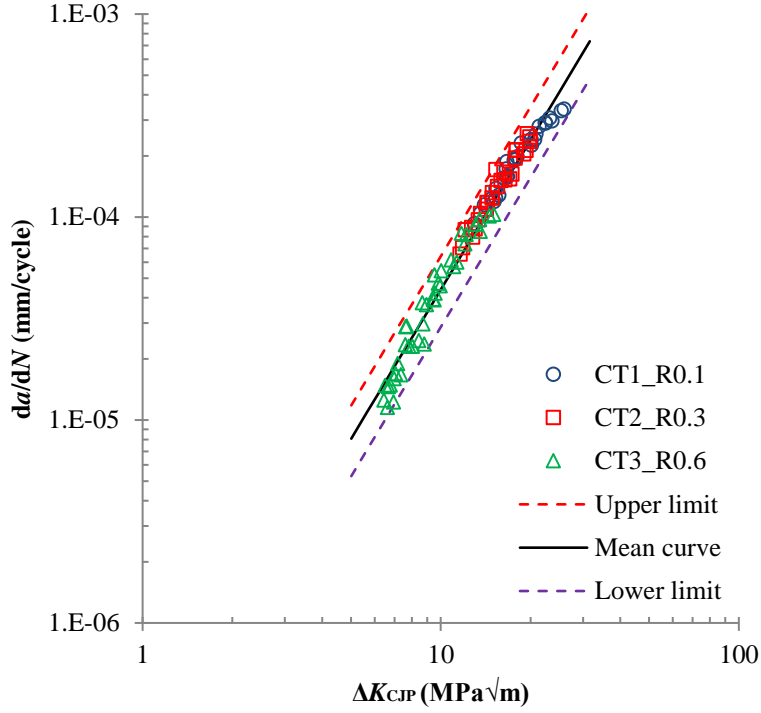
independent parameter.

(a)

(b)
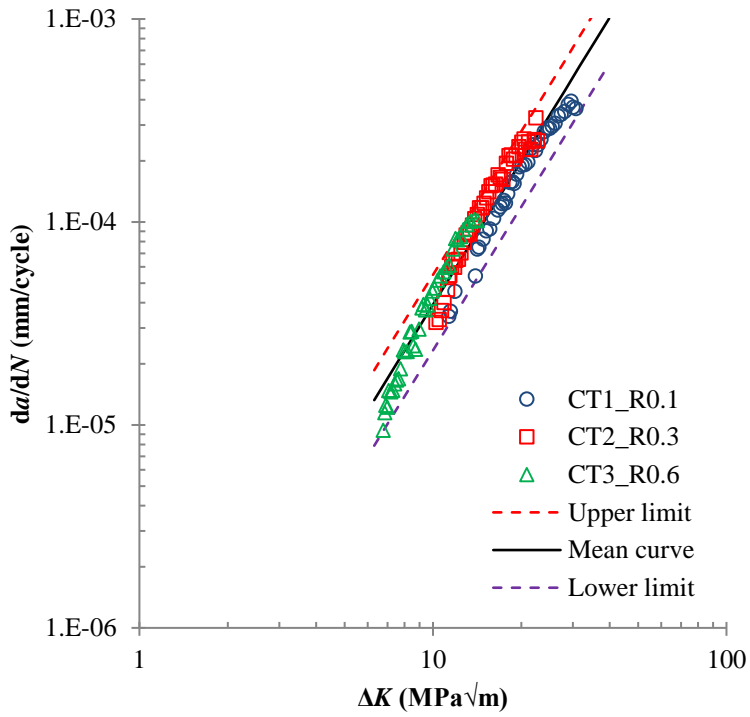
Fig. 7. Fatigue crack growth rate as a function of the stress intensity factor range for CT specimens. (a) da/dN-ΔK relation and (b) da/dN-ΔK_{CJP} relation.

To facilitate the comparisons between the fatigue crack growth rate relations, Paris law [4] is applied to calculate the crack growth rate curve. It can be linearized as following equations for the da/dN-ΔK relation and the da/dN-ΔK_{CJP} relation respectively,

$$\lg\left(\frac{\mathrm{d}a}{\mathrm{d}N}\right) = A' + B'\lg(\Delta K) \tag{6}$$

$$\lg\left(\frac{\mathrm{d}a}{\mathrm{d}N}\right) = A' + B'\lg(\Delta K_{\text{CJP}}) \tag{7}$$

where, A' and B' are constants which can be obtained by fitting the test data using the least square method. These two parameters can be calculated using the least square method and are listed in Table 4. The mean curve of the fatigue crack growth rate can also be drawn in Fig. 8. Besides the linear correlation coefficient, r, another two indexes are

introduced to reflect the degree of data dispersion comparing to the mean curve. That is, the sum of the distances between the test data and the mean curve, d_{sum}, and the maximum value of the distances, d_{max} (as illustrated in Fig. 8). The larger these two indexes are, the greater the data dispersion degree is. It can be drawn from Fig. 7 and Table 8 that both the da/dN-ΔK data and the da/dN-ΔK_{CJP} data show a highly linear relation, but the level of the data dispersion of da/dN-ΔK_{CJP} is smaller than that of da/dN-ΔK according to the values of all the indexes.

Table 8. Parameters of the mean fatigue crack growth rate curves and corresponding data dispersion indexes.

Specimen Type	da/dN-ΔK relation					da/dN-ΔK_{CJP} relation				
	A'	B'	r	d_{sum}	d_{max}	A'	B'	r	d_{sum}	d_{max}
CT	-6.7574	2.3498	0.9772	3.71	0.086	-6.8357	2.4819	0.9896	1.64	0.063
DEN	-6.8432	2.7234	0.9588	1.05	0.075	-6.3284	2.1117	0.9869	0.68	0.065
BOTH	-6.7429	2.4006	0.9173	7.83	0.182	-6.7536	2.4146	0.9898	2.32	0.066

$$d_{sum}=d_1+d_2+\ldots+d_6$$
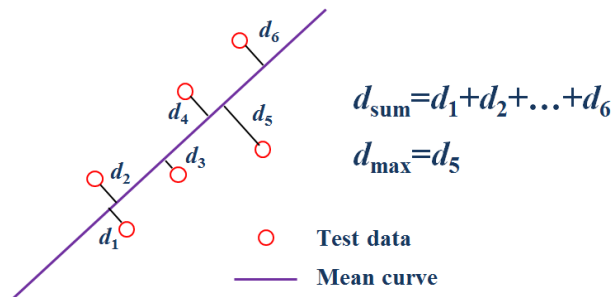$$d_{max}=d_5$$

○ Test data
—— Mean curve

Fig. 8. Illustration of the definitions of the two data dispersion indexes, d_{sum} and d_{max}.

2.2.2. The da/dN-ΔK and the da/dN-ΔK_{CJP} relations for DEN specimens

Similar to the analysis process of section 2.2.1, test data of the da/dN-ΔK and that of the da/dN-ΔK_{CJP} on log-log graphs, and relevant crack growth rate curves for DEN specimens are depicted in Fig. 9. Parameters of the mean fatigue crack growth rate curves and corresponding data dispersion indexes are also listed in Table 8. For the da/dN-ΔK relation

of DEN specimens, it exhibits a more obvious effect of stress ratios on the distribution of

the test data, namely with given ΔK, the crack growth rate is higher at R=0.3 than that at

R=0.05. This phenomenon is more distinct than that happens to CT specimens. But once

replace the standard stress intensity factor range with ΔK_{CJP}, the test data obtained by

using two different DEN specimens at two different stress ratios overlaps with each other

again. The dispersion indexes of the test data obtained from DEN specimens in Table 8

also prove the much higher linearization degree of da/dN-ΔK_{CJP} relation.
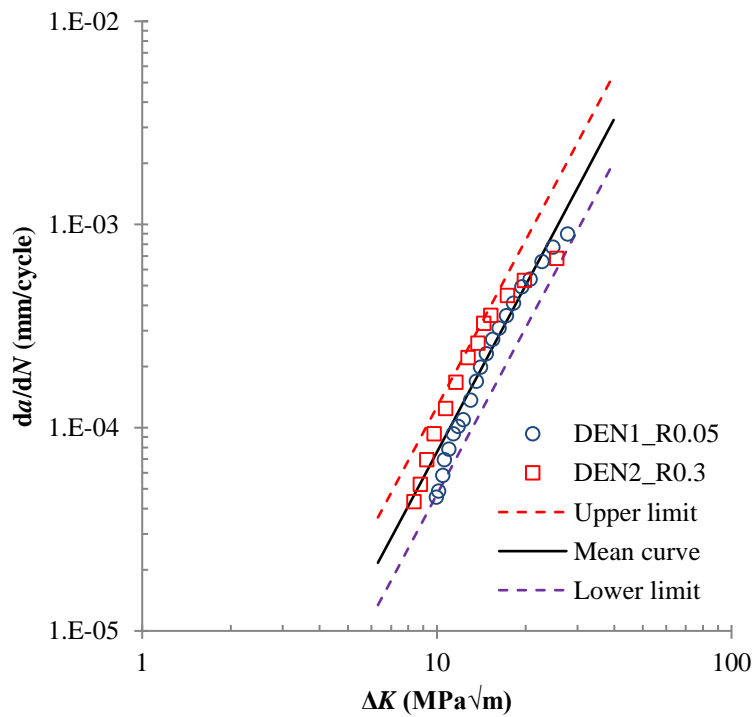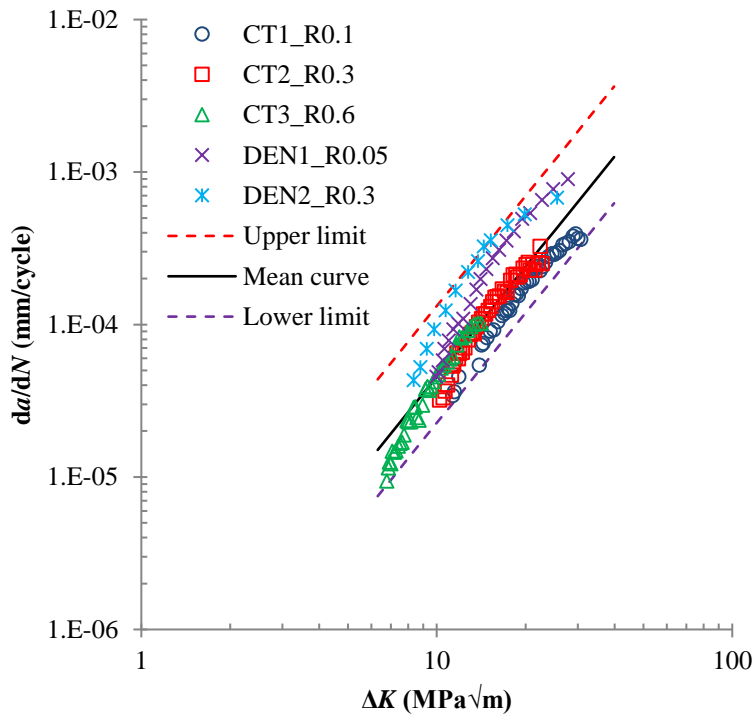

(a)
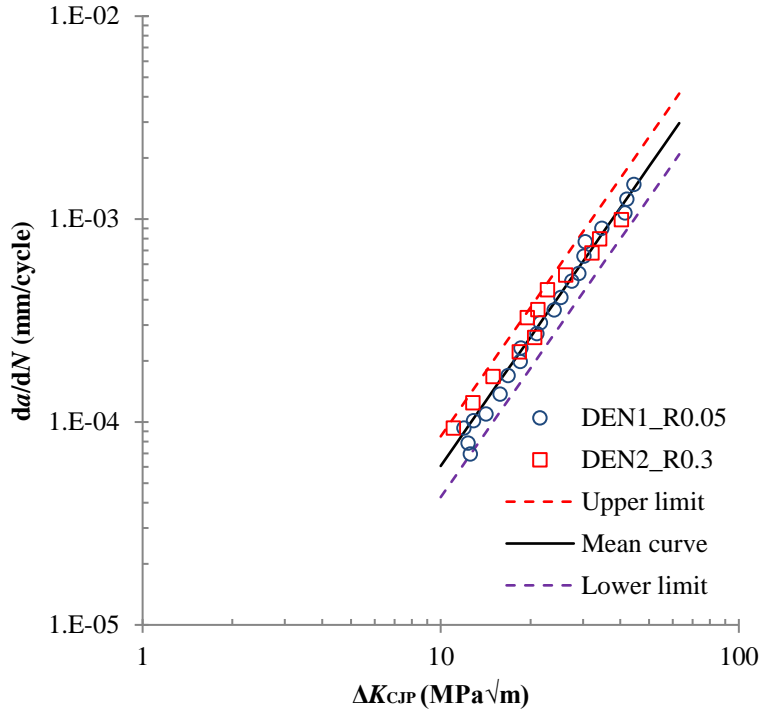
(b)

Fig. 9. Fatigue crack growth rate as a function of the stress intensity factor range for DEN specimens. (a) da/dN-ΔK relation and (b) da/dN-ΔK_{CJP} relation.

2.2.3. The da/dN-ΔK and the da/dN-ΔK_{CJP} relations for both kinds of specimens

Fig. 10 shows the test data of the da/dN-ΔK and that of the da/dN-ΔK_{CJP} for both the CT specimens and the DEN specimens on log-log graphs, while the data dispersion indexes are still included in Table 8. It is quite obvious that due to the high geometry-sensitivity of the da/dN-ΔK relation, when test data obtained by using different kinds of specimens are drawn together, the data dispersion gets tremendous large. Linear equation is no longer suggested for fitting the test data. The linear correlation coefficient, r, is only 0.9173 while the d_{sum} and the d_{max} are both much larger than those for the CT or the DEN specimens alone. The change of local stress condition near the crack tip introduced by the difference of specimen geometries can explain the large dispersion of test data and therefore the

traditional stress intensity factor range ΔK, is incapable of depicting the fatigue crack growth rate without considering the specimen geometries. Fortunately, the CJP model-based stress intensity factor range, ΔK_{CJP}, shows its instinctive specimen geometry-independent characteristic and once again describes the crack growth rate data by using different specimens and at different stress ratios with a rather straight line. The test data in Fig. 10b distributes along this line in a narrow-band and the linear correlation coefficient, r, is up to 0.9898, while the d_{sum} and the d_{max} are only 29.6% and 36.3% of those for da/dN-ΔK relation. All these indicate that ΔK_{CJP} is applicable for a more effective rationalisation of fatigue crack growth rate for various specimen geometries and tress ratios.

(a)
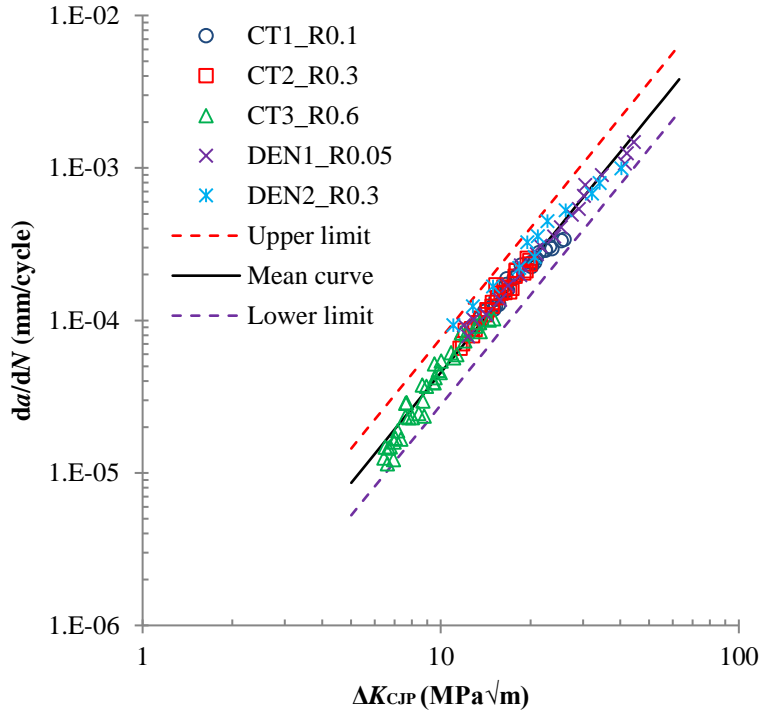
(b)

Fig. 10. Fatigue crack growth rate as a function of the stress intensity factor range for both the CT and the DEN specimens. (a) da/dN-ΔK relation and (b) da/dN-ΔK_{CJP} relation.

3. Calibration curves for relating ΔK_{CJP} to ΔK

As mentioned and analyzed above, the CJP model was specifically developed to obtain an elastic stress field model that explicitly captures the influences of an embedded region of plasticity surrounding a growing fatigue crack. It provides a better characterisation of the forces and stresses that arise from the plastic enclave around a crack and the lead to plasticity-induced shielding. The stress intensity factor range, ΔK_{CJP}, which is derived based on this model, is believed to act as a more intrinsic parameter obtained directly from the displacement fields near the crack tip to describe the fatigue crack growth behaviour. In other words, for certain material there could be only one da/dN-ΔK_{CJP} equation which can make the fracture analysis and the safety assessment much more convenient. For the

commercially pure grade 2 titanium used in this study, the da/dN-ΔK_{CJP} equation is listed

in Table 8 and can be expressed as:

$$\lg\left(\frac{da}{dN}\right) = -6.7536 + 2.4146\lg\left(\Delta K_{CJP}\right) \tag{8}$$

However, it's not easy to do calculations of ΔK_{CJP} without actually testing a specimen,

which has blocked the further application of the CJP model. A possible solution is, as in the

early days of fracture mechanics, it should be possible to obtain calibration curves for

particular geometries of specimen that would allow calculating the constants in the CJP

model from the curves and the equations related to standard ΔK. Then, ΔK_{CJP} can be

calculated easily with the function indirectly depends on ΔK so that the da/dN-ΔK_{CJP}

equation can play an efficient role in fatigue analysis. This section introduces the process

of the establishment of above mentioned calibration curves.

3.1. Expression of ΔK_{CJP} using constants in the CJP model

In the CJP model, K_F and K_R are given by:

$$K_F = \sqrt{\frac{\pi}{2}}\left(A - 3B + 8D\right) \tag{9}$$

$$K_R = \sqrt{\frac{\pi}{2}} \times 4D\pi \tag{10}$$

where, A, B and D are constants in the CJP model. Therefore, K_F-K_R can be expressed as:

$$K_F - K_R = \sqrt{\frac{\pi}{2}}\left(A - 3B - 4.566D\right) \tag{11}$$

Accordingly, equation 5 can be rewritten as following expression by introducing equation

11 into it rationally:

$$\Delta K_{CJP} = \sqrt{\frac{\pi}{2}} \left(\Delta A - 3\Delta B - 4.566\Delta D \right)$$

$$= 1.253\Delta A - 3.759\Delta B - 5.721\Delta D \tag{12}$$

3.2. Relation establishment between ΔK_{CJP} and ΔK

It's not difficult to imagine if the calibration curves between the standard ΔK and the constants range, ΔA, ΔB and ΔD, in the CJP model can be determined, then ΔK_{CJP} is also related to ΔK. According to the test data, ΔA, ΔB and ΔD as a function of standard ΔK for the CT specimens and for the DEN specimens are illustrated in Fig. 11. It's obvious that the data distribution of the ΔA, ΔB, ΔD vs. the ΔK for CT specimens show highly linear relations. Therefore, the linear equation should be appropriate to describe the calibration curves. However, it's not the case for DEN specimens. Instead, the quadratic equation in one unknown is more suitable to be taken as the calibration curves.
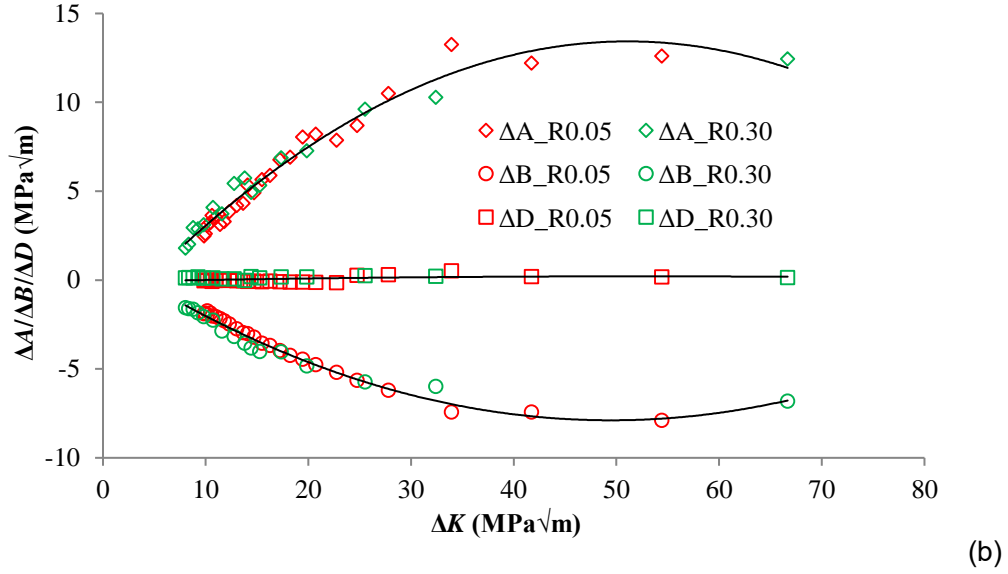

(a)

(b)
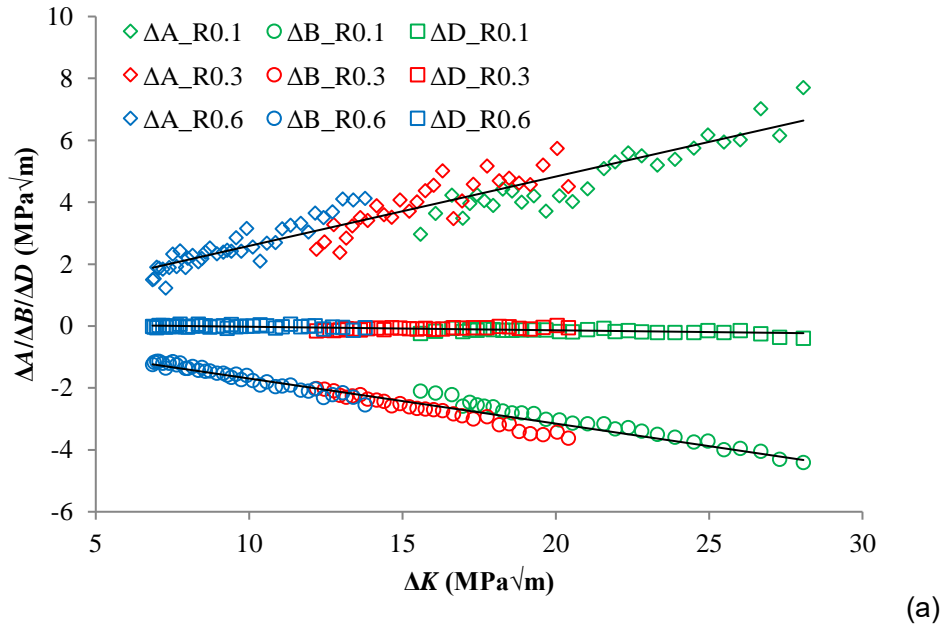
Fig. 11. ΔA, ΔB and ΔD as a function of standard ΔK for (a) the CT specimens and for (b) the DEN specimens.

By fitting the data in Fig. 11a, calibration curves for the CT specimens can be obtained and listed as follows:

$$\Delta A = 0.2241\Delta K + 0.3474$$

$$\Delta B = -0.1456\Delta K - 0.2399 \qquad (13)$$

$$\Delta D = -0.0114\Delta K + 0.0914$$

Similarly, according to the data in Fig. 11b, calibration curves for the DEN specimens can be fitted as follows:

$$\Delta A = 0.2241\Delta K + 0.3474$$

$$\Delta B = -0.1456\Delta K - 0.2399 \qquad (14)$$

$$\Delta D = -0.0114\Delta K + 0.0914$$

Thus, by plugging equation 13 and equation 14 into equation 12 respectively, the relations between the ΔK_{CJP} and the ΔK for the CT specimens and for the DEN specimens of present

commercially pure titanium alloy can be written as:

For CT specimen: $\Delta K_{\mathrm{CJP}} = 0.8885\Delta K + 0.8553$ (15)

For DEN specimen: $\Delta K_{\mathrm{CJP}} = -0.0213\Delta K^2 + 2.1235\Delta K - 7.6856$ (16)

Fig. 12 shows the calculated ΔK_{CJP} data using DIC technique as a function of ΔK for the CT specimens and for the DEN specimens respectively and also illustrates the corresponding prediction curves using equation 15 and equation 16. It is clear the prediction curves have quite good fitting effect to the test data. Now that the relations between the ΔK_{CJP} and the ΔK have been constructed, the da/dN-ΔK_{CJP} equation (equation 8) which is based on the CJP model can be utilized in the fatigue analysis for present CT and DEN specimens with any given ΔK value.
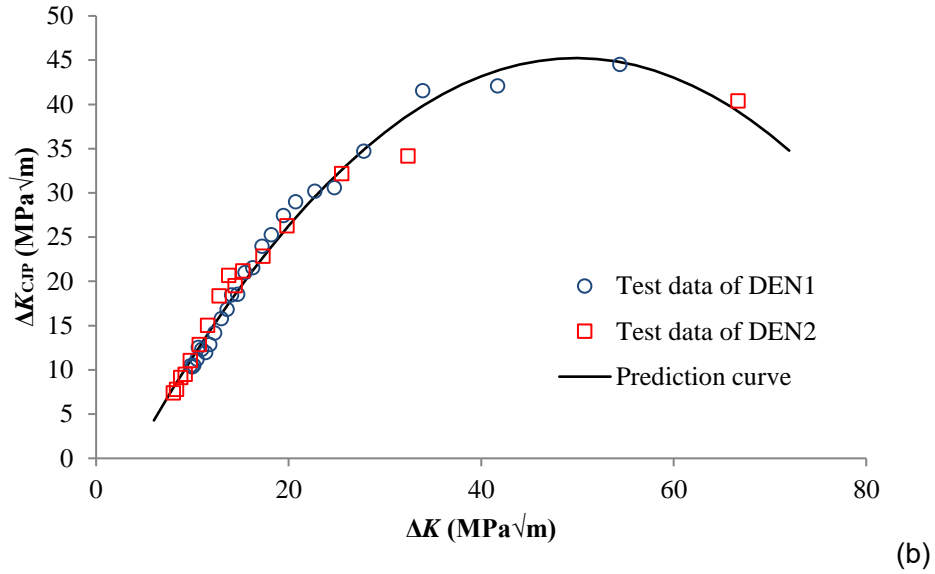

(a)

(b)
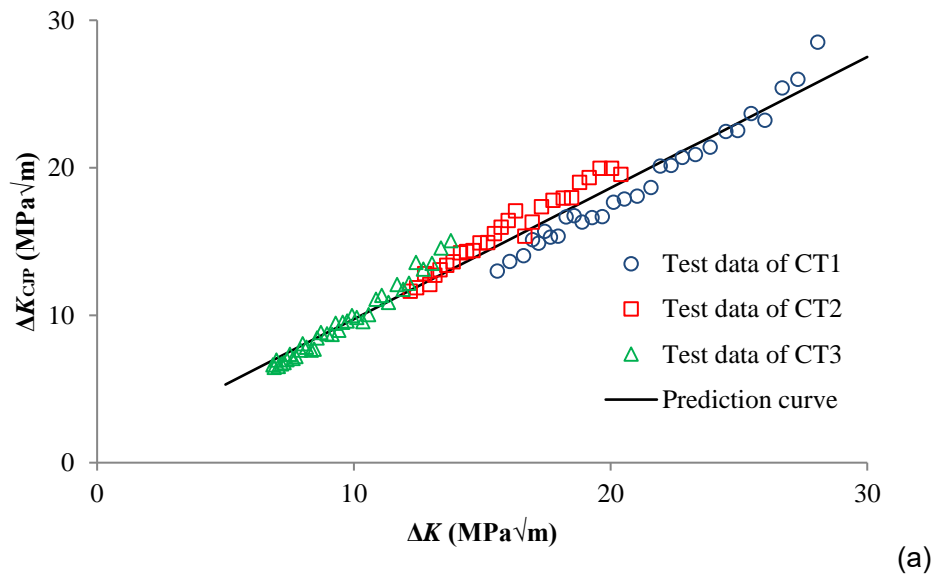
Fig. 12. Calculated ΔK_{CJP} values using DIC technique as a function of ΔK and corresponding prediction curves for (a) the CT specimens and for (b) the DEN specimens.

As an example, when the crack length, a, is 15.06 mm for specimen CT1, the ΔK value can be calculated using equation 3 and is 13.333 MPa√m. Then plug this ΔK value into equation 15 and get the corresponding ΔK_{CJP} value to be 12.702 MPa√m (while the ΔK_{CJP} value obtained from the DIC analysis is 12.900 MPa√m). Furthermore, by using the da/dN-ΔK_{CJP} equation as expressed in equation 8, the crack growth rate can be determined to be 8.193×10^{-5} mm/cycle (while the da/dN value obtained from the test data by utilizing five-point approximation method is 9.251×10^{-5} mm/cycle). Therefore, the calibration curves obtained in this section provide an effective way to promote the applications of the CJP model and relevant da/dN-ΔK_{CJP} equation.

Conclusions

Based on the fatigue crack growth rate tests using Grade 2 titanium CT specimens and

DEN specimens at different stress ratios (0.1, 0.3 and 0.6 for CT specimens while 0.05 and 0.3 for DEN specimens), the crack tip displacement fields were measured by utilizing the DIC technique. Then the distribution of the fatigue crack growth rate data, da/dN, as a function of the Irwin ΔK-value and of the CJP model-based ΔK_{CJP}-value on log-log coordinate graphs were comparatively analysed. Different from the standard ΔK which is quite sensitive both to the stress-ratio and to the specimen geometry, ΔK_{CJP} shows its distinct stress ratio-independent and geometry-independent characteristics. The relation between $\lg(da/dN)$ and $\lg(\Delta K_{CJP})$ of the titanium in this study for various specimen geometries and stress ratios can be depicted using one straight line function, and the test data distributes along this line in a narrow-band. The linear correlation coefficient is up to 0.9898 while the two dispersion indexes, d_{sum} and d_{max}, are only 29.6% and 36.3% of those for da/dN-ΔK relation. In fact, the linear equation is no longer suitable for fitting the test data of the fatigue crack growth rate vs. the standard ΔK in this case. Furthermore, the calibration curves for relating the constants in the CJP model to standard ΔK were obtained. For the CT specimens the curves are some linear equations, while for the DEN specimens they are described well with quadratic equations. The applications of the CJP model and the relevant da/dN-ΔK_{CJP} equation were then promoted by relating ΔK_{CJP} to ΔK by using above calibration curves. This study has actually proved that ΔK_{CJP} is obtainable through constructing some calibration curves, and it is capable for a more effective rationalisation of fatigue crack growth rate for various specimen geometries and tress ratios.

Acknowledgements

References

[1] Tada H, Paris PC, Irwin GR. The stress analysis of cracks handbook. New York: ASM International, 2000: p. 61.

[2] S Al Laham. Stress Intensity Factor and Limit Load Handbook. British Energy Generation Ltd, Issue 2, 1998: AI. 46.

[3] James MN, Christopher CJ, Díaz FA, Vasco-Olmo JM, Kakiuchi T, Patterson EA. Interpretation of plasticity effects using the CJP crack tip field model. Solid State Phenomena, 2017, 258: 117-124.

[4] Paris P, Erdogan F. A critical analysis of crack propagation laws. J. Basic Eng. Trans. ASME, 1963: 528-534.